

# Evidence for cell surface association between CXCR4 and ganglioside GM3 after gp120 binding in SupT1 lymphoblastoid cells

Maurizio Sorice<sup>a</sup>, Tina Garofalo<sup>a</sup>, Roberta Misasi<sup>a</sup>, Agostina Longo<sup>a</sup>, Vincenzo Mattei<sup>a</sup>,  
Patrizio Sale<sup>a</sup>, Vincenza Dolo<sup>b</sup>, Roberto Gradini<sup>a</sup>, Antonio Pavan<sup>b,\*</sup>

<sup>a</sup>Dipartimento di Medicina Sperimentale e Patologia, Università di Roma 'La Sapienza', Viale Regina Elena 324, Rome 00161, Italy

<sup>b</sup>Dipartimento di Medicina Sperimentale, Università di L'Aquila, Via Vetoio Coppito 2, L'Aquila 67100, Italy

Received 31 July 2001; accepted 14 August 2001

First published online 14 September 2001

Edited by Felix Wieland

**Abstract** CXCR4 (fusin) is a chemokine receptor which is involved as a coreceptor in gp120 binding to the cell surface. In this study we provide evidence that binding of gp120 triggers CXCR4 recruitment to glycosphingolipid-enriched microdomains. Scanning confocal microscopy showed a nearly complete localization of CXCR4 within GM3-enriched plasma membrane domains of SupT1 cells and coimmunoprecipitation experiments revealed that CXCR4 was immunoprecipitated by IgG anti-GM3 after gp120 pretreatment. These findings reveal that gp120 binding induces a strict association between CXCR4 and ganglioside GM3, supporting the view that GM3 and CXCR4 are components of a functional multimolecular complex critical for HIV-1 entry. © 2001 Published by Elsevier Science B.V. on behalf of the Federation of European Biochemical Societies.

**Key words:** GM3; Ganglioside; CXCR4; gp120; Microdomain

## 1. Introduction

Gangliosides, sialic acid-containing glycosphingolipids, are ubiquitous constituents of cell membranes [1], where they show cell type-specific expression patterns. In human lymphoblastoid cells, monosialoganglioside GM3 is the main ganglioside constituent of cell plasma membrane, since it represents about 70% of the total ganglioside content [2]. Previous studies revealed a clustered distribution of GM3 molecules on the cell surface of human peripheral blood lymphocytes (PBL), as well as of lymphoblastoid T cell lines [3]. Further analysis indicated that GM3 represents one of the main markers of glycosphingolipid-enriched microdomains (GEM) [4,5] which are referred to lipid rafts described in several cell types [6,7]. We identified these specialized portions of cell plasma membrane in human PBL as low density Triton X-100-insoluble fraction due to their poor solubility in cold non-ionic detergents [3]. Gangliosides in these fractions may be involved in

modulating signal transduction, mainly by interaction with specific signal transducer molecules detected in these domains [8], which include tyrosine kinase receptors, mono- (Ras, Rap) and heterotrimeric G proteins, Src-like tyrosine kinases (lck, lyn, fyn), protein kinase C (PKC) isozymes and glycosylphosphatidylinositol (GPI) anchored proteins [9–11]. We previously demonstrated that, in lymphocytes, CD4 and p56<sup>lck</sup>, a member of the Src family of tyrosine kinases, are selectively recovered in GM3-enriched microdomains [3,5]. Moreover, in human T lymphocytes exogenous GM3 induces CD4 phosphorylation [12], dissociation from p56<sup>lck</sup> and internalization via endocytic pits and vesicles [13].

HIV-1 infects T lymphocytes by binding to the CD4 receptor, followed by gp120–gp41-mediated fusion of viral and target cell membranes [14]. In addition to CD4, several members of the chemokine receptor family act as coreceptors for HIV-1 fusion and infection. The initial interaction with CD4 induces a conformational change in gp120, which promotes the interaction with the chemokine receptors CXCR4 (fusin) and CCR5, the main HIV coreceptors. Specific gangliosides, including Gb3 and GM3, are crucial elements in organizing gp120–gp41, CD4 and chemokine receptors into a membrane fusion complex [15]. On the basis of the demonstration that (a) microdomains play an essential role in the HIV-1-induced lateral associations required for viral infection [15,16], (b) a physical association between CXCR4 and the CD4–gp120 complex was observed in human cell lines [17], and (c) the HIV coreceptor CCR5 was found in lipid rafts [18], we investigated CXCR4 association with GEM, by evaluating its interaction with GM3, the main ganglioside constituent of these microdomains.

## 2. Materials and methods

### 2.1. Cells

The human T cell line SupT1, expressing human CXCR4, was maintained in RPMI-1640, containing 10% fetal calf serum (FCS), 2 mM glutamine, 100 U/ml penicillin and 0.1 mg/ml streptomycin (PenStrep).

### 2.2. Immunoelectron microscopy

SupT1 cells, fixed in 2% formaldehyde in phosphate-buffered saline (PBS) for 30 min at 4°C, were incubated with the anti-CXCR4 monoclonal antibody (mAb) 12G5 (R&D Systems, Inc., Minneapolis, MN, USA) for 1 h at 4°C. After washing, cells were incubated with gold-conjugated goat anti-mouse IgG (10 nm) (Sigma Chem. Co, St Louis, MO, USA). Control experiments were performed omitting the mAb from the immunolabeling procedure. All samples were fixed with 2%

\*Corresponding author. Fax: (39)-862-433523.  
E-mail address: pavan@univaq.it (A. Pavan).

**Abbreviations:** PBL, peripheral blood lymphocytes; GEM, glycosphingolipid-enriched microdomains; PKC, protein kinase C; GPI, glycosylphosphatidylinositol; FCS, fetal calf serum; HPTLC, high performance thin layer chromatography; mAb, monoclonal antibody; SDS-PAGE, sodium dodecyl sulfate–polyacrylamide gel electrophoresis; PBS, phosphate-buffered saline; HRP, horseradish peroxidase; FITC, fluorescein isothiocyanate

glutaraldehyde, post-fixed in 1% osmium tetroxide, dehydrated in ethanol and embedded in Epon 812. Samples were then sectioned, post-stained with uranyl acetate and lead citrate, and examined under an electron microscope (Philips CM10, Eindhoven, The Netherlands).

### 2.3. Ganglioside extraction

Ganglioside extraction was performed according to the method of Svennerholm and Fredman [19], with minor modifications. Briefly, cells were extracted twice in chloroform:methanol:water (4:8:3 by volume) and subjected to Folch partition by the addition of water to give a final chloroform:methanol:water ratio of 1:2:1.4. The upper phase, containing polar glycosphingolipids, was desalted and low molecular weight contaminants were removed using Supelclean LC-18 tubes (Supelco, Bellefonte, PA, USA), according to the method of Williams and McCluer [20]. The eluted glycosphingolipids were dried and separated by high performance thin layer chromatography (HPTLC), using silica gel 60 HPTLC plates (Merck, Darmstadt, Germany). Chromatography was performed in chloroform:methanol:0.25% aqueous KCl (5:4:1) (v:v:v). Plates were air-dried and gangliosides visualized with resorcinol [21].

### 2.4. Isolation of GEM fractions

GEM fractions were isolated as previously described [22]. Briefly,  $2 \times 10^8$  SupT1 cells, incubated in the presence or in the absence of recombinant gp120 (Intracel, Seattle, WA, USA), 10  $\mu\text{g}/\text{ml}$ , for 30 min at 37°C, were suspended in 1 ml of lysis buffer containing 1% Triton X-100, 10 mM Tris-HCl (pH 7.5) 150 mM NaCl, 5 mM EDTA, 1 mM  $\text{NaVO}_4$ , and 75 U of aprotinin and allowed to stand for 20 min. The cell suspension was mechanically disrupted by Dounce homogenization (10 strokes). The lysate was centrifuged for 5 min at  $1300 \times g$  to remove nuclei and large cellular debris. The

supernatant fraction (postnuclear fraction) was subjected to sucrose density gradient centrifugation, i.e. the fraction was mixed with an equal volume of 85% sucrose (w/v) in lysis buffer (10 mM Tris-HCl, pH 7.5 150 mM NaCl, 5 mM EDTA). The resulting diluent was placed at the bottom of a linear sucrose gradient (5–30%) in the same buffer and centrifuged at  $200\,000 \times g$  for 16–18 h at 4°C in a SW41 rotor (Beckman Instruments, Palo Alto, CA, USA). After centrifugation, the gradient was fractionated, and 11 fractions were collected starting from the top of the tube. All steps were done at 0–4°C. The amount of protein in each fraction was first quantified, by Bio-Rad protein assay (Bio-Rad Lab. GmbH, Munich, Germany). Finally, all fractions were subjected to sodium dodecyl sulfate–polyacrylamide gel electrophoresis (SDS–PAGE) (10% acrylamide). The proteins were electrophoretically transferred to nitrocellulose (Bio-Rad, Hercules, CA, USA) and then, after blocking with PBS containing 1% albumin, probed with rabbit IgG anti-CXCR4 (Sigma) or anti-CD4 (Santa Cruz Biotechnology, Santa Cruz, CA, USA). Bound antibodies were visualized with horseradish peroxidase (HRP)-conjugated anti-rabbit IgG (Sigma) and immunoreactivity assessed by chemiluminescence reaction using the ECL Western blocking detection system (Amersham, Buckinghamshire, UK).

### 2.5. Analysis of GM3–CXCR4 colocalization on the cell surface of SupT1 by scanning confocal microscopy

SupT1 cells were suspended in RPMI and 10% fetal bovine serum ( $5 \times 10^7$  cells/ml), incubated in the presence or in the absence of recombinant gp120 (Intracel), 10  $\mu\text{g}/\text{ml}$ , for 30 min at 37°C and then washed at 4°C in PBS. Cells were then fixed with 4% formaldehyde in PBS for 30 min at 4°C and labeled with 12G5 anti-CXCR4 mAb (R&D Systems) for 1 h at 4°C, followed by addition (30 min at 4°C) of Texas red-conjugated anti-mouse IgG (Calbiochem-Novabio-

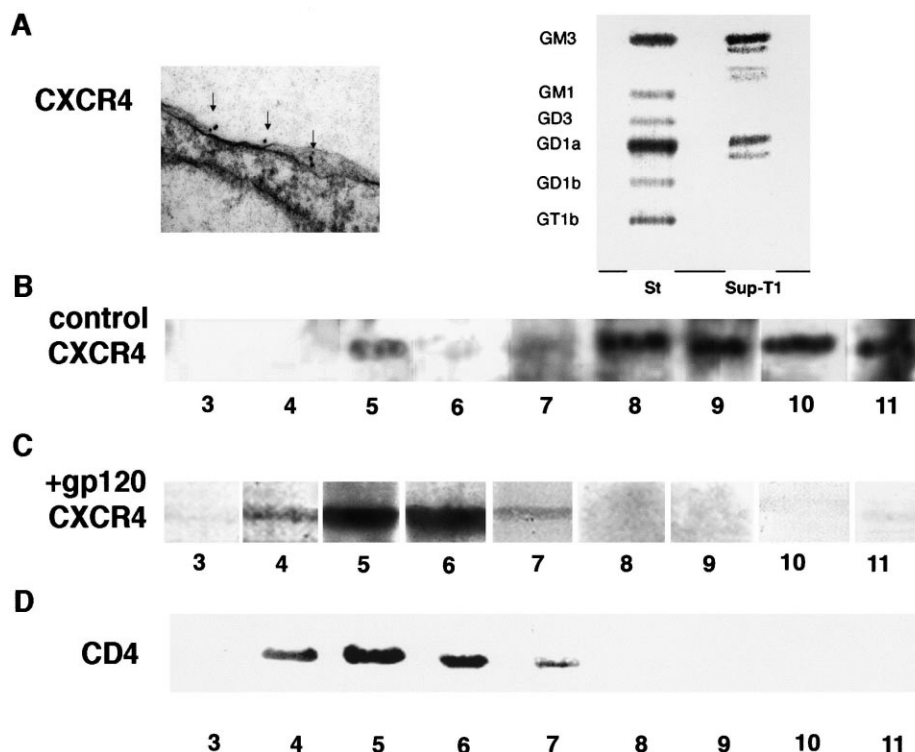


Fig. 1. A: Left, immunolabeling of CXCR4 molecules on SupT1 plasma membrane. Right: HPTLC analysis of the ganglioside pattern of SupT1 cells. Gangliosides were extracted in chloroform–methanol–water. The plate was stained with resorcinol. B: CXCR4 distribution in control SupT1 sucrose gradient fractions. SupT1 were lysed in lysis buffer and the supernatant fraction (postnuclear fraction) was subjected to sucrose density gradient. After centrifugation the gradient was fractionated, and each gradient fraction was recovered and analyzed by Western blotting with anti-CXCR4 Ab. C: CXCR4 distribution in gp120 pretreated (10  $\mu\text{g}/\text{ml}$ , for 30 min at 37°C) SupT1 sucrose gradient fractions. SupT1 were lysed in lysis buffer and the supernatant fraction (postnuclear fraction) was subjected to sucrose density gradient. After centrifugation the gradient was fractionated, and each gradient fraction was recovered and analyzed by Western blotting with anti-CXCR4 Ab. D: CD4 distribution in SupT1 sucrose gradient fractions. SupT1 cells were lysed in lysis buffer and the supernatant fraction (postnuclear fraction) was subjected to sucrose density gradient. After centrifugation the gradient was fractionated, and each gradient fraction was recovered and analyzed by Western blotting with anti-CD4 Ab.

chem, La Jolla, CA, USA). After three washes in PBS, cells were incubated with GMR6 anti-GM3 mAb [23], a gift from Dr. T. Tai, Tokyo Metropolitan Institute of Medical Science, Tokyo, Japan, for 1 h at 4°C, followed by three washes in PBS and addition (30 min at 4°C) of fluorescein isothiocyanate (FITC)-conjugated goat anti-mouse IgM (Sigma). In parallel experiments, cells were stained with anti-GM3 mAb before fixing the cells. Cells were finally washed three times in PBS and resuspended in glycerol/Tris-HCl pH 9.2. The images were acquired through a confocal laser scanning microscope Zeiss LSM 510 (Zeiss, Oberkochen, Germany) equipped with Argon Ion and HeNe laser. Simultaneously, the green (FITC) and the red (Texas red, which reduces overlapping greatly) fluorophores were excited at 488 nm and 518 nm. Acquisition of single FITC-stained samples in dual fluorescence scanning configuration did not show contribution of green signal in red. Images were collected at  $1024 \times 1024$  pixels.

## 2.6. Coimmunoprecipitation of GM3 and CXCR4 in SupT1 cells

Coimmunoprecipitation of GM3 and CXCR4 was performed according to Iwabuchi et al. [24]. Briefly, SupT1 cells, treated with recombinant gp120 (Intracel) for 30 min, as above, were lysed in lysis buffer (20 mM HEPES, pH 7.2/ 1% Nonidet P-40/ 10% glycerol/50 mM NaF/1 mM phenylmethylsulfonyl fluoride/1 mM  $\text{Na}_3\text{VO}_4$ /10  $\mu\text{g}$  of leupeptin per ml). Cell-free lysates (containing 20–25  $\mu\text{g}$  of protein) were mixed with protein A-acrylic beads and stirred by a rotary shaker for 2 h at 4°C to pre-clear non-specific binding. After centrifugation ( $500 \times g$  for 1 min), the supernatant was added with 20  $\mu\text{l}$  of anti-GM3 mAb DH2 (IgG3) ascites [25] (a gift from Dr. A. Prinetti, Department of Medical Chemistry and Biochemistry, University of Milan, Milan, Italy) or with mouse IgG with irrelevant specificity (Sigma), as a negative control. The mixtures were placed overnight in a rotary mixer at 4°C, added with protein A-acrylic beads and placed again in a rotary mixer for 2 h. Beads were washed three times with PBS containing 0.01% Tween 20, by brief weak centrifugation ( $500 \times g$  for 1 min) and then suspended in sample buffer with mercaptoethanol, heated to 95°C for 3 min, and centrifuged ( $1000 \times g$  for 2 min). After SDS-PAGE with 10% polyacrylamide gels and transfer to nitrocellulose membrane (Bio-Rad, Hercules, CA, USA) the supernatants were probed with polyclonal anti-CXCR4 (Sigma). Bound antibodies were then visualized with HRP-conjugated anti-rabbit IgG

(Sigma) and immunoreactivity assessed by chemiluminescence reaction using the ECL Western blocking detection system (Amersham, Buckinghamshire, UK). Densitometric scanning analysis was performed by Mac OS 9.0 (Apple Computer International), using NIH Image 1.62 software.

## 3. Results

### 3.1. CXCR4 distribution on SupT1 cell plasma membrane

To investigate the cell surface distribution of CXCR4 an ultrastructural analysis was performed directly on SupT1 cells. Fig. 1A (left) shows CXCR4 immunolabeling on the cell plasma membrane, evidenced by gold-conjugated anti-IgG antibodies.

### 3.2. Ganglioside pattern of SupT1 cells

High-performance thin-layer chromatography analysis of

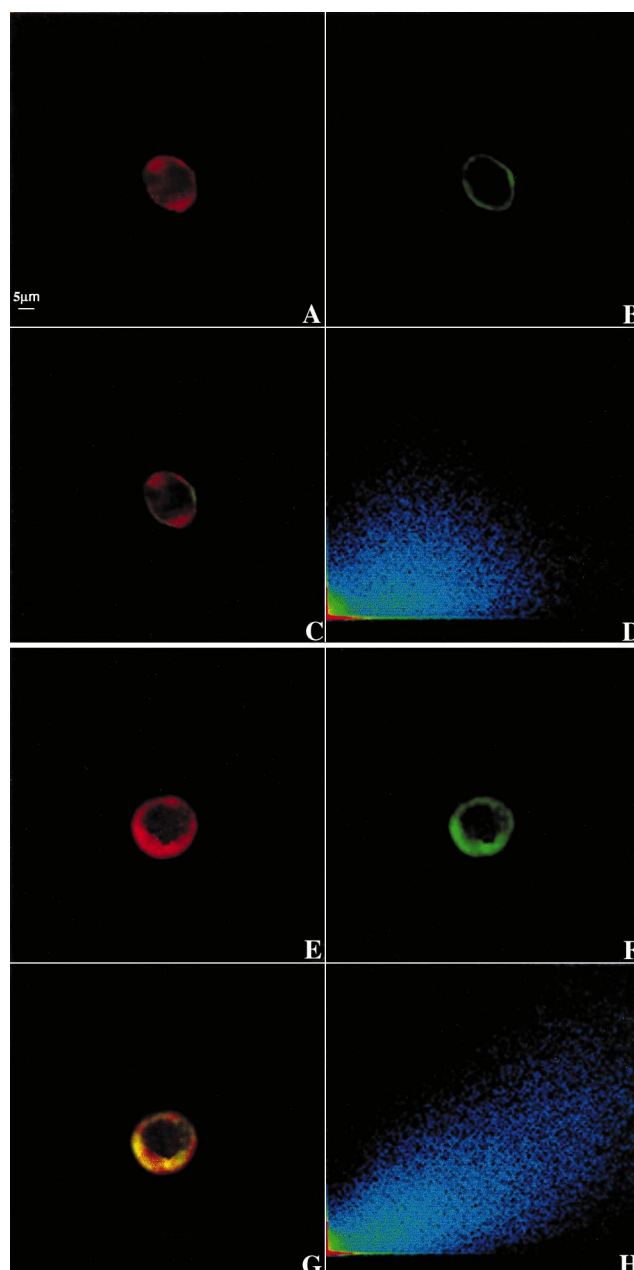


Fig. 2. Scanning confocal microscopic analysis of GM3-CXCR4 association on SupT1 plasma membrane after gp120 binding. Cells were labeled with anti-CXCR4 mAb, followed by the addition of Texas red-conjugated anti-mouse IgG. Cells were then incubated with anti-GM3 (GMR6), followed by the addition of FITC-conjugated goat anti-mouse IgM. Scale bar: 5  $\mu\text{m}$ . A: Untreated cells stained with anti-CXCR4, followed by the addition of Texas red-conjugated anti-mouse IgG. B: Untreated cells stained with anti-GM3, followed by the addition of FITC-conjugated anti-mouse IgM. C: Dual immunolabeling of anti-GM3 (green) and anti-CXCR4 (red) on untreated cells. Colocalization areas are stained in yellow. D: Two-dimensional scatter plot analysis of the dual-labeled fluorochromes (pseudocolor) GM3-CXCR4. Diagrams show the pixel intensity distribution of a dual-channel section. The x-axis represents intensity from the red channel; the y-axis represents intensity from the green channel; a low colocalization is well evident, since the area of interest is not only the red-green area, but also the blue area, which should be taken into consideration as far as the number of colocalized pixels is concerned. E: Cells pretreated with gp120 (10  $\mu\text{g}/\text{ml}$ , for 30 min at 37°C), stained with anti-CXCR4, followed by the addition of Texas red-conjugated anti-mouse IgG. F: Cells pretreated with gp120 (10  $\mu\text{g}/\text{ml}$ , for 30 min at 37°C), stained with anti-GM3, followed by the addition of FITC-conjugated anti-mouse IgG. G: Dual immunolabeling of anti-GM3 (green) and anti-CXCR4 (red) on cells pretreated with gp120 (10  $\mu\text{g}/\text{ml}$ , for 30 min at 37°C). Colocalization areas are stained yellow. H: Two-dimensional scatter plot analysis of the dual-labeled fluorochromes (pseudocolor) GM3-CXCR4. Diagrams show the pixel intensity distribution of a dual-channel section. The x-axis represents intensity from the red channel; the y-axis represents intensity from the green channel; a major colocalization index is evident, since the blue area is larger and more directed towards the diagonal line.

acidic glycosphingolipids extracted from SupT1 cells revealed the presence of the following resorcinol bands: a main GM3 comigrating band and two other bands, migrating between GM3 and GM1, and with GD1a (Fig. 1A, right). The ganglioside double bands are due to the heterogeneity of fatty acid composition, as described [26]. Gb3 was not detectable.

### 3.3. CXCR4 recruitment to GEM after pretreatment with gp120

To better define the distribution of CXCR4 on the cell surface, we investigated the presence of CXCR4 in GEM fractions of SupT1 obtained by a 5–30% linear sucrose gradient, in the absence or in the presence of gp120 (10 µg/ml for 30 min at 37°C). The results revealed that only a small amount of CXCR4 was detectable in the fraction 5, corresponding to GEM of cell plasma membrane. The higher amount of CXCR4 was detected in Triton-soluble fractions (fractions 8–11) (Fig. 1B). On the contrary, CD4 was present in the fractions 4, 6, 7, but also in fraction 5, where it appeared highly enriched (Fig. 1D), as previously reported [3,4]. In cells treated with gp120 the higher amount of CXCR4 was detected in the Triton-insoluble fractions (Fig. 1C), indicating that gp120 induced CXCR4 recruitment to GEM.

### 3.4. Association between GM3 and CXCR4 in SupT1 after pretreatment with gp120

In order to study the possible GM3–CXCR4 interaction in SupT1 cells, we analyzed their distribution on the plasma membrane (Fig. 2A,B). The results by scanning confocal microscopy revealed that most of the cells showed an uneven signal distribution of ganglioside molecules over the cell surface (Fig. 2B). In order to determine the possible association between CXCR4 and MG3, we superimposed the double immunostaining of anti-CXCR4 and anti-GM3 in the absence or in the presence of gp120 (30 min at 37°C). In the absence of gp120, GM3 and CXCR4 show weak colocalization (Fig. 2C). This finding suggests that GM3 and CXCR4 are not physically associated in the absence of gp120. In the presence of gp120 (Fig. 2E,F) the merged image of anti-CXCR4 and anti-GM3 staining revealed yellow areas, resulting from overlap of green and red fluorescence, which correspond to nearly complete colocalization areas (Fig. 2G). Scatter plot diagrams of the corresponding images showed graphically how the dual labels are colocalized. Fig. 2D showed two distinct clusters, indicating weak GM3–CXCR4 colocalization. Fig. 2H showed a single cluster of high pixel values, indicating that, after gp120 binding, CXCR4 molecules were mainly, but not exclusively, localized in membrane domains enriched with GM3 molecules.

### 3.5. Coimmunoprecipitation of GM3 and CXCR4 in SupT1 after pretreatment with gp120

We analyzed the association between GM3 and CXCR4 in the absence or in the presence (30 min at 37°C) of gp120. Lysates from SupT1 cells were immunoprecipitated with DH2 anti-GM3 mAb, followed by protein A–Sepharose beads. GM3 and its possible complex with associated proteins were eluted from the beads and subjected to Western blotting, using a rabbit polyclonal anti-CXCR4 Ab. With this approach, a tiny band was detected in the immunoprecipitates from untreated cells (Fig. 3A, lane b), indicating that only few CXCR4 molecules were present in the GM3 immunoprecipi-

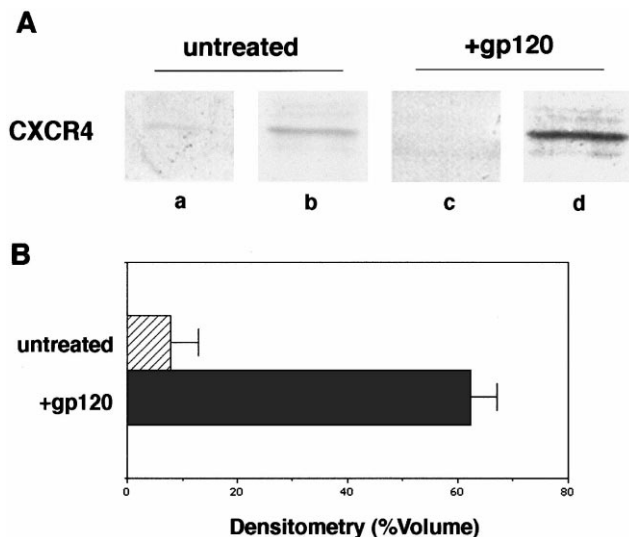


Fig. 3. A: Coimmunoprecipitation of GM3 and CXCR4 in SupT1 cells: Western blot analysis of GM3 immunoprecipitate. SupT1 were lysed in lysis buffer. Cell-free lysates were normalized for proteins and immunoprecipitated with IgG anti-GM3 mAb (DH2). Proteins from the immunoprecipitate were separated on 10% SDS-PAGE and probed with the anti-CXCR4 polyclonal Ab. Lane a: irrelevant IgG immunoprecipitate on untreated SupT1 cells. Lane b: GM3 immunoprecipitate on untreated SupT1 cells. Lane c: irrelevant IgG immunoprecipitate on gp120 pretreated SupT1 cells (10 µg/ml, for 30 min at 37°C). Lane d: GM3 immunoprecipitate on gp120 pretreated SupT1 cells (10 µg/ml, for 30 min at 37°C). B: Densitometric scanning analysis of the immunoblotting with anti-CXCR4 Ab on GM3 immunoprecipitates (mean of five experiments). Arbitrary units.

tate. In cells treated with gp120 (Fig. 3A, lane d) an about 8-fold increase of CXCR4 band was observed, as detected by densitometric analysis (Fig. 3B). This finding demonstrates that gp120 binding on the cell surface of SupT1 cells induces an association between CXCR4 and ganglioside GM3. In control samples the immunoprecipitation with a mouse IgG with irrelevant specificity, under the same condition, did not result in detectable levels of CXCR4 (Fig. 3A, lanes a and c, respectively).

## 4. Discussion

In this report we demonstrated that gp120 binding triggers CXCR4 recruitment to GM3-enriched microdomains in SupT1 cells, a lymphoblastoid T cell line in which GM3 is the main ganglioside constituent and Gb3 is not detectable. This finding is in agreement with the preliminary observation of Symington and Hakomori [27], who observed that Gb3 is not expressed by T cells but is the major neutral GSL in macrophages. On the other hand, it is well known that exogenous Gb3 is able to restore the fusion activity of HIV-1 [15]. Interestingly, the glycosylation pattern of gp120 used in this study is identical to that of the natural human protein. It is very important, since glycosylation of gp120 is a prerequisite for binding to the host cell CD4 and deglycosylation abolishes or impairs the binding [28].

In order to define the receptor distribution, we preliminary investigated the presence of CXCR4 on the cell surface by immunoelectron microscopy and in GEM fractions by immunoblotting. In our previous observations, we demonstrated

that in human lymphocytes GM3, CD4 and p56<sup>lck</sup> are selectively recovered in these domains where they form a stable complex [3,5]. Our present findings indicated that CXCR4 is not enriched as much as CD4 in GEM fraction of SupT1 cells. This finding does not appear surprising, since it was observed that antibody to CD4 did not coimmunoprecipitate CXCR4 from human cell lines [17]. Moreover, these results concur with the reported poor association between CD4 and CXCR4, observed by Xiao et al. [29]. In addition, the different constitutive endocytosis rates of CD4 and CXCR4 expressed on SupT1 cells [30], the absence of comodulation of CXCR4ΔCyt with CD4 on phorbol ester-treated Mv-1Lu cells [31], and the selective SDF-1-induced down-modulation of CXCR4 but not CD4 [31], argued against the possibility that these two proteins do normally form stable associations.

Interestingly, the main finding of this study is represented by the observation that gp120 binding on the cell surface of SupT1 cells induces CXCR4 recruitment to GEM, where the receptor is associated with the GEM-specific component ganglioside GM3. Indeed, scanning confocal microscopical images supported the existence of GM3-enriched microdomains on the surface of SupT1 lymphoblastoid cells, where CXCR4 molecules were mainly, but not exclusively, colocalized with GM3. In the present study the GM3–CXCR4 association after gp120 pretreatment was also demonstrated by a novel approach, showing that CXCR4 was coimmunoprecipitated by an IgG anti-GM3 (DH2) [25]. This procedure represents, in our hand, a valuable tool that led us to clarify the role of GM3 as a transducer molecule, with the cooperation of specific proteins [5]. This approach was validated by the studies of Yamamura [32] and Iwabuchi [33], who revealed that in B16 melanoma cells the DH2 antibody immunoprecipitated multiple signal transducer molecules, such as c-Src, Rho and FAK. High affinity SDS-resistant ganglioside–protein interactions have been reported in different cell types and exert relevant functional effects [34–37]. Our findings parallel with evidence that CXCR4 is recruited into a molecular complex with CD4–gp120 at the cell surface [17]. This association may stabilize the post-binding conformational state of the gp120–41 envelope required for exposure of the gp41 hydrophobic NH<sub>2</sub>-terminus and its insertion into the target membrane. Our new findings suggest a role for gangliosides as structural components of the multimolecular signaling complex involved in gp120 binding on the cell surface. It is substantially in agreement with the recent observation that gp120 induces the lateral reorganization of rafts, bringing the CD4–gp120 complexes together with rafts containing the chemokine receptor [16]. This hypothesis is further supported by the demonstration that raft integrity is required for lateral assembly of CD4–gp120 complexes with the CXCR4 and for fusion of the HIV-1 envelope and the cell plasma membrane [16]. Taken together, these findings provide evidence that CD4–gp120 binding triggers CXCR4 recruitment to GEM, suggesting that GM3, CD4, CXCR4 and, possibly, CCR5, are components of a multimolecular organization critical for virus entry. The role of the ganglioside in this multimolecular system could be to facilitate the migration of the CD4–gp120 complex to an appropriate coreceptor, such as CXCR4, since CD4 and coreceptor are not physically associated in the absence of HIV-1 [17]. In conclusion, the data presented here indicate that these plasma membrane GEM may be a target for new strategies to prevent or block HIV-1 infection.

**Acknowledgements:** We thank Professor Tadashi Tai, Tokyo Metropolitan Institute of Medical Science, Tokyo, Japan, for providing us with the IgM anti-GM3 GMR6, Dr. Alessandro Prinetti, Department of Medical Chemistry and Biochemistry, University of Milan, for providing us the IgG anti-GM3 DH2 and Dr. Mark Marsh, University College, London, for helpful suggestions and critical reading of the manuscript. This work was supported by Grants from Ministero dell'Università e della Ricerca Scientifica e Tecnologica (MURST), Consiglio Nazionale della Ricerche (CNR) (no. 98.00515.CT04) and Ministero del lavoro e della Previdenza no. 792.

## References

- [1] Hakomori, S. (1981) *Annu. Rev. Biochem.* 50, 733–764.
- [2] Kiguchi, K., Henning-Chubb, B.C. and Huberman, E. (1990) *J. Biochem.* 107, 8–14.
- [3] Sorice, M., Parolini, I., Sansolini, T., Garofalo, T., Dolo, V., Sargiacomo, M., Tai, T., Peschle, C., Torrisi, M.R. and Pavan, A. (1997) *J. Lipid Res.* 38, 969–980.
- [4] Parolini, I., Topa, S., Sorice, M., Pace, A., Ceddia, P., Montessoro, E., Pavan, A., Lisanti, M.P., Peschle, C. and Sargiacomo, M. (1999) *J. Biol. Chem.* 274, 14176–14187.
- [5] Sorice, M., Garofalo, T., Misasi, R., Longo, A., Mikulak, J., Dolo, V., Pontieri, G.M. and Pavan, A. (2000) *Glycoconj. J.* 17, 247–252.
- [6] Jacobson, K. and Dietrich, C. (1999) *Trends Cell Biol.* 9, 87–91.
- [7] Simons, K. and Ikonen, E. (1997) *Nature* 387, 569–572.
- [8] Hakomori, S., Handa, K., Iwabuchi, K., Yamamura, S. and Prinetti, A. (1998) *Glycobiology* 8, XI–XIX.
- [9] Parolini, I., Sargiacomo, M., Lisanti, M.P. and Peschle, C. (1996) *Blood* 87, 3783–3794.
- [10] Stefanova, I. and Horejsi, V. (1991) *J. Immunol.* 147, 1587–1592.
- [11] Horejsi, V., Drbal, K., Cebecauer, M., Cerny, J., Brdicka, T., Angelisova, P. and Stockinger, H. (1999) *Immunol. Today* 20, 356–361.
- [12] Garofalo, T., Sorice, M., Misasi, R., Cinque, B., Giammatteo, M., Pontieri, G.M., Cifone, M.G. and Pavan, A. (1998) *J. Biol. Chem.* 273, 35153–35160.
- [13] Sorice, M., Pavan, A., Misasi, R., Sansolini, T., Garofalo, T., Lenti, L., Pontieri, G.M., Frati, L. and Torrisi, M.R. (1995) *Scand. J. Immunol.* 41, 148–156.
- [14] Dimitrov, D. (1997) *Cell* 91, 721–730.
- [15] Hug, P., Lin, H.M.J., Korte, T., Xiao, X., Dimitrov, D.F., Wang, J.M., Puri, A. and Blumenthal, R. (2000) *J. Virol.* 74, 6377–6385.
- [16] Manes, S., del Real, G., Lacalle, R.A., Lucas, P., Gomez-Mouton, C., Sanchez-Palomino, S., Delgado, R., Alami, J., Mira, E. and Martinez-A, C. (2000) *EMBO Rep.* 1, 190–195.
- [17] Lapham, C.K., Ouyang, J., Chandrasekhar, B., Nguyen, N.Y., Dimitrov, D.S. and Golding, H. (1996) *Science* 274, 602–605.
- [18] Manes, S., Mira, E., Gomez-Mouton, C., Lacalle, R.A., Keller, K., Labrador, J.P. and Martinez-A, C. (1999) *EMBO J.* 18, 6211–6220.
- [19] Scennerholm, L. and Fredman, P. (1980) *Biochim. Biophys. Acta* 617, 97–109.
- [20] Williams, M.A. and McCluer, R.H. (1980) *J. Neurochem.* 35, 266–269.
- [21] Svennerholm, L. (1957) *Biochim. Biophys. Acta* 24, 604–611.
- [22] Rodgers, W. and Rose, J.K. (1996) *J. Cell Biol.* 135, 1515–1523.
- [23] Kotani, M., Ozawa, H., Kawashima, I., Ando, S. and Tai, T. (1992) *Biochim. Biophys. Acta* 1117, 97–103.
- [24] Iwabuchi, K., Handa, K. and Hakomori, S.I. (2000) *Methods Enzymol.* 312, 488–494.
- [25] Dohi, T., Nores, G. and Hakomori, S. (1988) *Cancer Res.* 48, 5680–5685.
- [26] Sekine, M., Ariga, T., Miyatake, T., Kuroda, Y., Suzuki, A. and Yamakawa, T. (1984) *J. Biochem.* 95, 155–160.
- [27] Symington, F.W. and Hakomori, S.I. (1985) *Lymphokines* 12, 201–238.
- [28] Matthews, T.J., Weinhold, K.J., Lyerly, H.K., langlois, A.J., Wigzell, H. and Bolognesi, D.P. (1987) *Proc. Natl. Acad. Sci. USA* 84, 5424–5428.
- [29] Xiao, X., Wu, L., Stantchev, T.S., Feng, Y.R., Ugolini, S., Chen, H., Shen, Z., Riley, J.L., Broder, C.C. and Settentau, Q.J. (1999) *Proc. Natl. Acad. Sci. USA* 96, 7496–7501.

- [30] Pelchen-Matthews, A., Armes, J.E., Griffiths, G. and March, M. (1991) *J. Exp. Med.* 173, 575–587.
- [31] Signoret, N., Oldridge, J., Pelchen-Matthews, A., Klasse, P.J., Tran, T., Brass, L.F., Rosenkilde, M.M., Schwartz, T.W., Holmes, W., Dallas, W., Luther, M.A., Wells, T.N.C., Hoxie, J.A. and March, M. (1997) *J. Cell Biol.* 139, 651–664.
- [32] Yamamura, S., Handa, K. and Hakomori, S. (1997) *Biochem. Biophys. Res. Commun.* 236, 218–222.
- [33] Iwabuchi, K., Yamamura, S., Prinetti, A., Handa, K. and Hakomori, S.I. (1998) *J. Biol. Chem.* 273, 9130–9138.
- [34] Misasi, R., Sorice, M., Garofalo, T., Griggi, T., Campana, W.M., Giammatteo, M., Pavan, A., Hiraiwa, M., Pontieri, G.M. and O'Brien, J.S. (1998) *J. Neurochem.* 71, 2313–2321.
- [35] Mutoh, T., Tokuda, A., Miyadai, T., Hamaguchi, M. and Fujiki, N. (1995) *Proc. Natl. Acad. Sci. USA* 92, 5087–5091.
- [36] Minoguchi, K., Swaim, W.D., Berenstein, E.H. and Siraganian, R.P. (1994) *J. Biol. Chem.* 269, 5249–5254.
- [37] Kasahara, K., Watanabe, Y., Yamamoto, T. and Sanai, Y. (1997) *J. Biol. Chem.* 272, 29947–29953.